Golubev, D. S.; Kirsanov, N. S.; Tan, Z. B.; Laitinen, A.; Galda, A.; Vinokur, V. M.; Haque, M.; Savin, A.; Lesovik, G. B.; Hakonen, P. J.

Nonlocal thermoelectricity in a hybrid superconducting graphene device

Published in:
MIPT (PHYSTECH) - QUANT 2020

DOI:
10.1063/5.0054927

Published: 16/06/2021

Document Version
Publisher's PDF, also known as Version of record

Nonlocal thermoelectricity in a hybrid superconducting graphene device

Cite as: AIP Conference Proceedings **2362**, 030003 (2021); https://doi.org/10.1063/5.0054927
Published Online: 16 June 2021

D. S. Golubev, N. S. Kirsanov, Z. B. Tan, A. Laitinen, A. Galda, V. M. Vinokur, M. Haque, A. Savin, G. B. Lesovik, and P. J. Hakonen

Nonlocal Thermoelectricity in a Hybrid Superconducting Graphene Device

D. S. Golubev,[1] N. S. Kirsanov,[2,3,4,5,a)] Z. B. Tan,[4,6] A. Laitinen,[4] A. Galda,[7,8] V. M. Vinokur,[8,5] M. Haque,[4] A. Savin,[4] G. B. Lesovik,[2,3] and P. J. Hakonen[4,1]

[1)] *QTF Centre of Excellence, Department of Applied Physics, Aalto University, FI-00076 Aalto, Finland*
[2)] *Terra Quantum AG, St. Gallerstrasse 16A, 9400 Rorschach, Switzerland*
[3)] *Moscow Institute of Physics and Technology, 141700, Institutskii Per. 9, Dolgoprudny, Moscow Distr., Russian Federation*
[4)] *Low Temperature Laboratory, Department of Applied Physics, Aalto University, Espoo, Finland*
[5)] *Consortium for Advanced Science and Engineering (CASE), University of Chicago, 5801 S Ellis Ave, Chicago, IL 60637, USA*
[6)] *Shenzhen Institute for Quantum Science and Engineering, and Department of Physics, Southern University of Science and Technology, Shenzhen 518055, China*
[7)] *James Franck Institute, University of Chicago, Chicago, IL 60637, USA.*
[8)] *Materials Science Division, Argonne National Laboratory, 9700 S. Cass Ave., Argonne, IL 60439, USA*

[a)] *Corresponding author: nikita.kirsanov@phystech.edu*

Abstract. The Seebeck effect producing voltage difference from temperature gradient has a wide spectrum of applications. Recent theoretical studies show that the Cooper pair splitting and the elastic co-tunneling can give rise to the nonlocal Seebeck effect in hybrid normal metal-superconductor-normal metal systems. Here we propose a coherent transport description of this nonlocal effect and validate its experimental observation in a graphene-based Cooper pair splitter.

INTRODUCTION

Quantum computation in solid state requires a robust source for entangled electrons. Splitting Cooper pairs of an *s*-wave superconductor may potentially provide such source. In the last two decades, significant progress towards this goal has been achieved. Cooper pair splitting (CPS) is usually studied in a setup with a bulk superconducting lead and two quantum dots attached to it, and its efficiency is characterized by the ratio of the current carried by the splitted pairs to the total current flowing through the dots. According to the theory, the efficiency of Cooper pair spitting can be improved, for example, by use of ferromagnetic leads [1], by Coulomb blockade effect [2], by presence of Majorana states in the quantum dots [3, 4, 5], and by energy filtering [6]. These predictions have been tested on several material platforms [7, 8, 9, 10, 11, 12, 13, 14], and particularly promising results have been obtained in carbon nanotube, graphene, and nanowire settings.

Along with the elastic co-tunneling (EC) process, the CPS establishes a new mechanism for thermoelectricity in hybrid superconducting systems [15, 16, 17, 18]. In this work, we present a coherent transport description of the nonlocal Seebeck effect originating from the temperature gradient across a quantum dot–superconductor–quantum dot splitter and compare our model with the experimental observations. Our work opens route for the devices enabling to generate entangled electrons in the situations where the thermal drive is more preferable than the electrical one.

COHERENT TRANSPORT MODEL

Let us introduce the theoretical description of the nonlocal thermoelectric effect in the graphene-based CPS device. The schematics of the device are presented in Fig. 1: two normal reservoirs are connected to the common superconductor (with the gap Δ) via two quantum dots; the nth energy level of the dot j ($j=\{L,R\}$ denotes the left and right dots) is $\varepsilon_{j,n}$. Each dot is coupled to the reservoir and superconductor with rate $\Gamma_{j,n}$ and $\gamma_{j,n}$, respectively. The temperatures of the left and right reservoirs and superconductor are, respectively, T_L, T_R and T_S. The resonance position of each dot can be tuned through the variation of the gate voltage $V_{sg,L(R)}$:

$$\varepsilon_{j,n}(V_{sg,j})=a_j(V_{sg,j}-V_{\max,j,n}),\quad \varepsilon'_{j,n}(V_{gj})=a_j(V_{sg,j}-V'_{j,n}), \tag{1}$$

where a_j is the constant determined by the gate and dot capacitances, $V_{\max,j,n}$ is the gate voltage corresponding to the maximum transmission probability of the dot, $V'_{j,n}$ is the gate voltage at which the energy $\varepsilon'_{j,n}$ of closely lying

MIPT (PhysTech) - QUANT 2020
AIP Conf. Proc. 2362, 030003-1–030003-6; https://doi.org/10.1063/5.0054927
Published by AIP Publishing. 978-0-7354-4102-6/$30.00

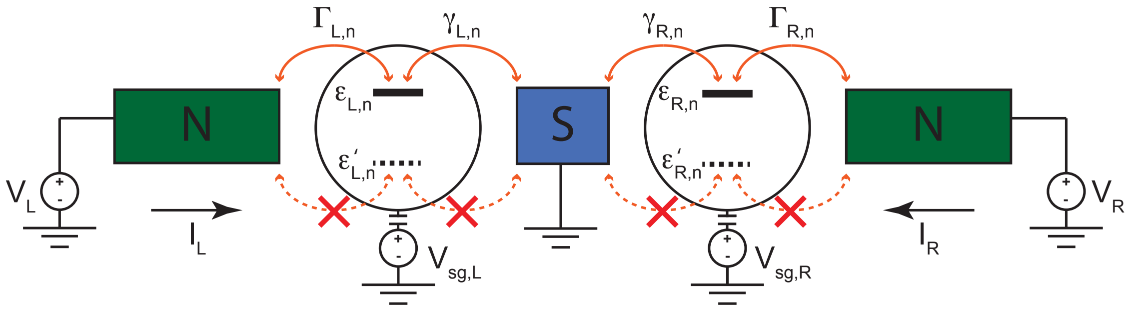

FIGURE 1. N-dot-S-dot-N hybrid system scheme. The normal reservoir j ($j = \{L, R\}$ denotes the left and right side) is coupled to the corresponding quantum dot with rate $\Gamma_{j,n}$ (n denotes the energy level); in turn, the dot is coupled to the superconductor with rate $\gamma_{j,n}$. The coupled energy levels $\varepsilon_{j,n}$ of the quantum dot j can be adjusted through changing the gate voltage $V_{sg,j}$ on the dot. In addition, the dots have dark energy levels $\varepsilon'_{j,n}$ uncoupled from the superconductor and normal reservoir which also depend on the gate voltage. The electrical current I_j flowing through the dot j is driven by the external bias voltages V_L and V_R on the left and right reservoirs (the superconductor is grounded) and the temperature differences in the structure.

uncoupled (dark) states is zero. We introduce the dark states to account for the possible Fano resonance effect which may significantly affect the conductance of the dots; the transmission probability of dot j is

$$\tau_j(E, V_{sg,j}) = \sum_n \frac{\gamma_{j,n}\Gamma_{j,n}}{\left(E - \varepsilon_{j,n}(V_{sg,j}) - \frac{|t_{j,n}|^2}{E - \varepsilon'_{j,n}(V_{sg,j})}\right)^2 + \frac{(\gamma_{j,n}+\Gamma_{j,n})^2}{4}}, \tag{2}$$

where $t_{j,n}$ is the hopping amplitude between $\varepsilon_{j,n}$ and dark $\varepsilon'_{j,n}$.

Temperature differences produce electric currents I_L and I_R flowing from the left and right reservoirs towards the superconductor. The current I_j is composed of the local (I_j^{loc}) and nonlocal (ΔI_j^{nl}) contributions:

$$I_L = I_L^{\mathrm{loc}} + \Delta I_L^{\mathrm{nl}}, \quad I_R = I_R^{\mathrm{loc}} + \Delta I_R^{\mathrm{nl}}. \tag{3}$$

The local contribution to the thermoelectric current is caused by the temperature difference between the corresponding normal reservoir and superconductor, while the nonlocal one arises from the temperature difference between two normal reservoirs. Let us now examine each contribution in more detail.

Local transport

The local transport through the individual dots can be described by the generalization of the Andreev reflection theory [19, 20] for the case of energy dependant transmission probabilities. Such case is discussed, for instance, in Ref. [21]; the results of this work can be translated into the following expressions for the local electric currents:

$$\begin{aligned} I_j^{\mathrm{loc}}(E, V_{sg,j}) = {} & \frac{e}{\pi\hbar}\int_{|E|<\Delta} dE \frac{\Delta^2[f_j(E-eV_j) - f_j(E+eV_j)]}{(\Delta^2 - E^2)\left[\left(\frac{2}{\tau_j(\tilde{E}_j, V_{sg,j})} - 1\right)\left(\frac{2}{\tau_j(-\tilde{E}_j, V_{sg,j})} - 1\right) - \frac{4\tilde{E}_j^2}{\Gamma_j^2(V_{sg,j})}\right] + E^2} \\ & + \frac{2e}{\pi\hbar}\int_{|E|>\Delta} dE \frac{\nu_S(E)\left(\frac{2}{\tau(-E, V_{sg,j})} - 1 + \nu_S(E)\right)[f_j(E-eV_j) - f_S(E)]}{\left(\frac{2}{\tau(-E, V_{sg,j})} - 1 + \nu_S(E)\right)\left(\frac{2}{\tau(E, V_{sg,j})} - 1 + \nu_S(E)\right) + \frac{4\Delta^2}{\Gamma_j^2(V_{sg,j})}\nu_S^2(E)}, \end{aligned} \tag{4}$$

where E is the energy of the incident particle, $f_j(E) = 1/(1 + e^{E/k_B T_j})$ is the distribution function in reservoir j, V_j is the bias voltage on the reservoir j (we are interested in the thermoelectric effect, therefore we will only consider the case where $V_L = V_R = 0$), $\nu_S(E) = \frac{|E|}{\sqrt{E^2 - \Delta^2}}$ is the density of states in the superconductor, and $\tilde{E}_j = E\sqrt{1 + \frac{\gamma_j(V_{sg,j})}{\sqrt{\Delta^2 - E^2}}}$ is the renormalised energy; we replaced the coupling rates $\Gamma_{j,n}$ $\gamma_{j,n}$ with functions $\Gamma_j(V_{sg,j})$ and $\gamma_j(V_{sg,j})$ depending on the gate voltage. From this expression we derive zero bias conductance of the dot j at low temperatures, $k_BT_j, k_BT_S \ll \Delta, \Gamma_{j,n}+\gamma_{j,n}$:

$$g_j(V_{sg,j}) = \frac{h}{e^2}\frac{\partial I_j}{\partial V_j}\bigg|_{V_j=0} = \frac{4\tau_j^2(0,V_{sg,j})}{(2-\tau_j(0,V_{sg,j}))^2}. \tag{5}$$

Nonlocal transport

The nonlocal transport through the NSN structure is governed by the CPS and EC processes occurring with probabilities $\tau_{\mathrm{CPS}}(E)$ and $\tau_{\mathrm{EC}}(E)$ respectively. As demonstrated in Refs. [2, 22, 23, 24], in the case where $\tau_{\mathrm{CPS}}(E)$, $\tau_{\mathrm{EC}}(E)$ $\ll 1$, these probabilities are given by simple formulae

$$\tau_{\mathrm{CPS}}(E) = \tau_L(E)\tau_S\tau_R(-E), \tag{6}$$

$$\tau_{\mathrm{EC}}(E) = \tau_L(E)\tau_S\tau_R(E), \tag{7}$$

where τ_S is the effective transmission probability of the superconductor. This parameter can be regarded as the probability that an electron incident from one dot reaches the opposite one rather than moving into the bulk of the superconductor. If the distance between the dots is less than the superconductor's coherence length, τ_S does not depend on E. The value of τ_S is determined by many factors, particularly the structure's geometry, connection between the dots and the superconductor, and the superconductor's granularity. In describing the experiment we will treat τ_S as a fitting parameter.

In the subgap regime, where k_BT_L, $k_BT_R \ll \Delta$, given that there is no external voltage bias on the reservoirs, $V_j = 0$, the nonlocal currents can be expressed in the Landauer form:

$$\begin{aligned}\Delta I_L^{\mathrm{nl}} &= \frac{e\tau_S}{h}\int dE\, \tau_L(E)\big\{\tau_R(E)+\tau_R(-E)\big\}\left[f_L(E)-f_R(E)\right],\\ \Delta I_R^{\mathrm{nl}} &= -\frac{e\tau_S}{h}\int dE\,\big\{\tau_L(E)+\tau_L(-E)\big\}\tau_R(E)\left[f_L(E)-f_R(E)\right].\end{aligned} \tag{8}$$

Given also that k_BT_L, $k_BT_R \ll \Delta$, $\gamma_{j,n}+\Gamma_{j,n}$, we can write the nonlocal currents in the form similar to Mott's formula,

$$\begin{aligned}\Delta I_L^{\mathrm{nl}} &= \frac{\pi^2}{3}\frac{ek_B^2}{h}\frac{\partial\tau_L(0,V_{sg,L})}{\partial E}\tau_S\tau_R(0,V_{sg,R})(T_L^2-T_S^2)\\ &= -\frac{\pi^2}{3}\frac{ek_B^2}{a_Lh}\tau_S\frac{\partial g_L(0,V_{sg,L})}{\partial V_{sg,L}}\frac{4\sqrt{g_R(V_{sg,R})}}{\sqrt{g_L(V_{sg,L})}\left(2+\sqrt{g_L(V_{sg,L})}\right)^2\left(2+\sqrt{g_R(V_{sg,R})}\right)}(T_L^2-T_S^2),\end{aligned} \tag{9}$$

$$\begin{aligned}\Delta I_R^{\mathrm{nl}} &= \frac{\pi^2}{3}\frac{ek_B^2}{h}\tau_L(0,V_{sg,L})\tau_S\frac{\partial\tau_R(0,V_{sg,R})}{\partial E}(T_R^2-T_S^2)\\ &= -\frac{\pi^2}{3}\frac{ek_B^2}{a_Rh}\tau_S\frac{\partial g_R(0,V_{sg,R})}{\partial V_{sg,R}}\frac{4\sqrt{g_L(V_{sg,L})}}{\sqrt{g_R(V_{sg,R})}\left(2+\sqrt{g_L(V_{sg,L})}\right)\left(2+\sqrt{g_R(V_{sg,R})}\right)^2}(T_R^2-T_S^2).\end{aligned} \tag{10}$$

Let us, for instance, analyze the behavior of the nonlocal current on the left, ΔI_L^{nl}. One may notice that ΔI_L^{nl} changes its sign when the left gate voltage $V_{sg,L}$ runs through the value corresponding to the extremum of the left dot's conductance $g_L(V_{sg,L})$. Meanwhile, the dependence of ΔI_L^{nl} on the right gate voltage $V_{sg,R}$ has a pattern qualitatively similar to the right dot's conductance $g_R(V_{sg,R})$. To this end, the nonlocal currents can be roughly described as $\Delta I_L^{\mathrm{nl}} \propto (dg_L/dV_{sg,L})g_R$, $\Delta I_R^{\mathrm{nl}} \propto g_L(dg_R/dV_{sg,R})$.

EXPERIMENT

Figure 2 displays our experimental setup. The Al superconducting Cooper pair injector overlays two graphene quantum dots. The resonance levels of the dots can be shifted independently by the side gate electrodes. To observe

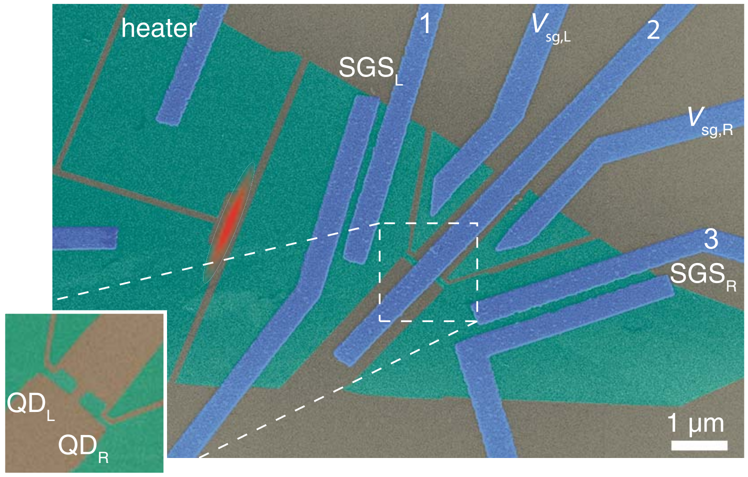

FIGURE 2. SEM image of the experimental device. The setup consists of graphene (green), metallic Al/Ti sandwich leads (blue) and silicon silicon wafer coated by 280 nm of silicon dioxide (gray). Red indicates the heated region. The superconducting lead 2 overlaps graphene quantum dots QD_L and QD_R with area 200×150 nm^2, shown in bottom left box. The transmission through the dots is determined by the voltages $V_{sg,L}$ and $V_{sg,R}$ on the graphene side gates. The superconductor-graphene-superconductor Josephson junctions are marked by SGS_L and SGS_R; leads 1 and 3 are connected to current preamplifiers and are used for thermoelectric measurements.

thermoelectricity, we create temperature gradient by means of a resistive graphene ribbon heater; the ribbon is connected to two aluminum electrodes, and the Joule heating from the ribbon is transmitted to the rest of the device through the silicon substrate. The heater is operated at frequency $f = 2.1$ Hz, thus the heating power $P = V_h^2/R$ (here, V_h is the heating voltage and R is the resistance of the ribbon) oscillates at double frequency $2f = 4.2$ Hz. In order to monitor the temperatures we use superconductor-graphene-superconductor (SGS) Josephson junctions: knowing the value of the switching current in the junction and its dependence on temperature we infer the local temperature. The arising thermoelectric currents flowing through the dots are recorded at frequency $2f = 4.2$ Hz by means of standard lock-in techniques.

To single out the nonlocal contribution $\Delta I_j^{\rm nl}$ from the measured total thermoelectric current I_j we notice that while $\Delta I_j^{\rm nl}$ depends on both gate voltages $V_{sg,L}$ and $V_{sg,R}$, the local contribution $I_j^{\rm loc}$ ideally depends only on $V_{sg,j}$. We also notice that $\Delta I_j^{\rm nl} \ll I_j^{\rm loc}$. Thus, one may say that $I_j^{\rm loc}$ is I_j averaged over the gate voltage on the opposite dot, making $\Delta I_j^{\rm nl}$ the small fast varying margin of the current. In reality, there is a cross talk between the dots, and the average background $\langle I_j(V_{sg,L}, V_{sg,R})\rangle$ should be determined differently: for dot j this background is obtained by fitting lines to the data matrix $I_j(V_{sg,L}, V_{sg,R})$ at constant $V_{sg,j}$ and then constructing a new matrix $\langle I_j(V_{sg,L}, V_{sg,R})\rangle$ using these line fits. Then, from experimental data we obtain the nonlocal contribution as

$$\Delta I_j^{\rm nl} = I_j(V_{sg,L}, V_{sg,R}) - \langle I_j(V_{sg,L}, V_{sg,R})\rangle. \tag{11}$$

The experimentally measured thermoelectric currents along with the theoretical predictions are shown in Fig. 3. The parameters of the theoretical model are such that they quite well fit the experimentally measured dots' conductance peaks while also correctly reflecting on the nonlocal current behavior. This combined agreement between the experiment and theory provides strong verification of the observed nonlocal Seebeck effect. For details see Ref. [25].

ACKNOWLEDGMENTS

We gratefully acknowledge C. Flindt, P. Burset, and T. Heikkilä for discussions and I. A. Sadovskyy for sharing his numerical codes. This work was supported by Aalto University School of Science Visiting Professor grant to G.B.L., as well as by Academy of Finland Projects No. 290346 (Z.B.T., AF post doc), No. 314448 (BOLOSE), and No. 312295 (CoE, Quantum Technology Finland). The work of A.L. was support by the Vilho, Yrjö and Kalle Väisälä Foundation of the Finnish Academy of Science and Letters. This work was also supported within the EU Horizon 2020 programme

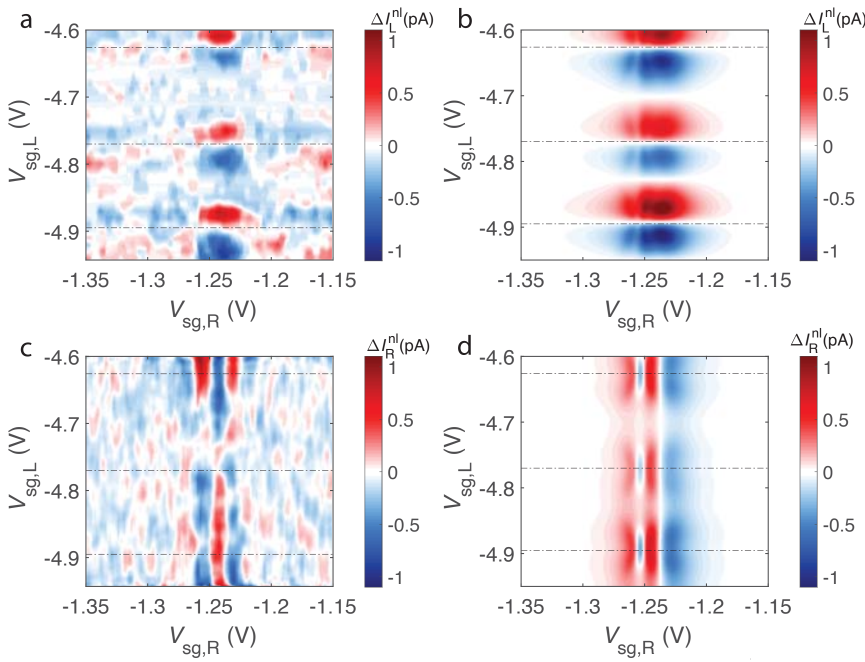

FIGURE 3. Nonlocal currents flowing through the left and right quantum dots as functions of the gate voltages on the dots. (a,c) Experimental plots. (b,d) Theoretical plots obtained using Eqs. (9) and (10). The parameters are such that they also enable good fitting of the conductance curves. The horizontal dotted lines correspond to the maximum conductance of the left dot.

by ERC (QuDeT, No. 670743), and in part by Marie-Curie training network project (OMT, No. 722923), COST Action CA16218 (NANOCOHYBRI), and the European Microkelvin Platform (EMP, No. 824109). The work of N.S.K. and G.B.L. was supported by the Government of the Russian Federation (Agreement No. 05.Y09.21.0018), by the RFBR Grants No. 17-02-00396A and No. 18-02-00642A, Foundation for the Advancement of Theoretical Physics and Mathematics BASIS, the Ministry of Education and Science of the Russian Federation No. 16.7162.2017/8.9. The work of N.S.K and A.G. at the University of Chicago was supported by the NSF grant DMR-1809188. The work of V.M.V. was supported by the U.S. Department of Energy, Office of Science, Basic Energy Sciences, Materials Sciences and Engineering Division.

REFERENCES

1. G. B. Lesovik, T. Martin, and G. Blatter, "Electronic entanglement in the vicinity of a superconductor," Eur. Phys. J. B **24**, 287–290 (2001).
2. P. Recher, E. V. Sukhorukov, and D. Loss, "Andreev tunneling, Coulomb blockade, and resonant transport of nonlocal spin-entangled elec-trons," Phys. Rev. B **63**, 165314 (2001).
3. J. Nilsson, A. R. Akhmerov, and C. W. J. Beenakker, "Splitting of a Cooper pair by a pair of Majorana bound states," Phys. Rev. Lett. **101**, 120403 (2008).
4. J. J. He, J. Wu, T.-P. Choy, X.-J. Liu, Y. Tanaka, and K. T. Law, "Correlated spin currents generated by resonant-crossed Andreev reflections in topological superconductors," Nature Commun. **5**, 3232 (2014).
5. Y.-T. Zhang, X. Deng, Q.-F. Sun, and Z. Qiao, "High-efficiency Cooper-pair splitter in quantum anomalous Hall insulator proximity-coupled with superconductor," Sci. Rep. **5**, 14862 (2015).
6. M. Veldhorst and A. Brinkman, "Nonlocal Cooper pair splitting in a pSn junction," Phys. Rev. Lett. **105**, 107002 (2010).
7. S. Russo, M. Kroug, T. M. Klapwijk, and A. F. Morpurgo, "Experimental observation of bias-dependent nonlocal Andreev reflection," Phys. Rev. Lett. **95**, 027002 (2005).
8. L. Hofstetter, S. Csonka, J. Nygård, and Schönenberger, "Cooper pair splitter realized in a two-quantum-dot Y-junction," Nature **461**, 960–963 (2009).
9. J. Wei and V. Chandrasekhar, "Positive noise cross-correlation in hybrid superconducting and normal-metal three-terminal devices," Nature Phys. **6**, 494–498 (2010).
10. J. Schindele, A. Baumgartner, and C. Schönenberger, "Near-unity Cooper pair splitting efficiency," Phys. Rev. Lett. **109**, 157002 (2012).
11. A. Das, Y. Ronen, M. Heiblum, D. Mahalu, A. V. Kretinin, and H. Shtrikman, "High-efficiency Cooper pair splitting demonstrated by two-particle conductance resonance and positive noise cross-correlation," Nature Commun. **3**, 1165 (2012).

12. R. S. Deacon, A. Oiwa, J. Sailer, S. Baba, Y. Kanai, K. Shibata, K. Hirakawa, and S. Tarucha, “Cooper pair splitting in parallel quantum dot Josephson junctions,” Nature Commun. **6**, 7446 (2015).
13. Z. B. Tan, D. D. Cox, T. Nieminen, P. Lähteenmäki, D. Golubev, G. B. Lesovik, and P. J. Hakonen, “Cooper pair splitting by means of graphene quantum dots,” Phys. Rev. Lett. **114**, 096602 (2015).
14. I. V. Borzenets, Y. Shimazaki, G. F. Jones, M. F. Craciun, S. Russo, M. Yamamoto, and S. Tarucha, “High efficiency CVD graphene-lead (Pb) Cooper pair splitter,” Sci. Rep. **6**, 23051 (2016).
15. Z. Cao, T.-F. Fang, L. Li, and H.-G. Luo, “Thermoelectric-induced unitary Cooper pair splitting efficiency,” Appl. Phys. Lett. **107**, 212601 (2015).
16. R. Sánchez, P. Burset, and A. L. Yeyati, “Cooling by Cooper pair splitting,” Physical Review B **98**, 241414 (2018).
17. R. Hussein, M. Governale, S. Kohler, W. Belzig, F. Giazotto, and A. Braggio, “Nonlocal thermoelectricity in a Cooper-pair splitter,” Physical Review B **99**, 075429 (2019).
18. N. S. Kirsanov, Z. B. Tan, D. S. Golubev, P. J. Hakonen, and G. B. Lesovik, “Heat switch and thermoelectric effects based on Cooper-pair splitting and elastic cotunneling,” Phys. Rev. B **99**, 115127 (2019).
19. G. E. Blonder, M. Tinkham, and T. M. Klapwijk, “Transition from metallic to tunneling regimes in superconducting micro-constrictions’ excess current, charge imbalance, and supercurrent conversion,” Phys. Rev. B **25**, 4515–4532 (1982).
20. C. W. J. Beenakker, “Quantum transport in semiconductor-superconductor microjunctions,” Phys. Rev. B **46**, 12841(R) (1992).
21. Q.-F. Sun, J. Wang, and T.-H. Lin, “Resonant Andreev reflection in a normal-metal-quantum-dot-superconductor system,” Phys. Rev. B **59**, 3831 (1999).
22. G. Deutscher and D. Feinberg, “Coupling superconducting-ferromagnetic point contacts by Andreev reflections,” Appl. Phys. Lett. **76**, 487–489 (2000).
23. D. S. Golubev, M. S. Kalenkov, and A. D. Zaikin, “Crossed Andreev reflection and charge imbalance in diffusive normal-superconducting-normal structures,” Physical Review Letters **103**, 067006 (2009).
24. D. S. Golubev and A. D. Zaikin, “Cross-correlated shot noise in three-terminal superconducting hybrid nanostructures,” Physical Review B **99**, 144504 (2019).
25. Z. B. Tan, A. Laitinen, N. S. Kirsanov, A. Galda, M. Haque, A. Savin, D. S. Golubev, V. M. Vinokur, G. B. Lesovik, and P. J. Hakonen, “Thermoelectric current in a graphene cooper pair splitter,” (2020), arXiv:2005.13286 [cond-mat.mes-hall].